

Supplementary Information for

A Universal Synthesis of Ultrathin Pd-Based Nanorings for Efficient Ethanol Electrooxidation

Yu Wang,^{a,†} Mengfan Li,^{a,†} Zhilong Yang,^{a,†} Wenchuan Lai,^a Jingjie Ge,^{b,c} Minhua Shao,^{b,c} Yu Xiang,^{d,*} Xuli Chen^{a,*} and Hongwen Huang^{a,*}

^a College of Materials Science and Engineering, Hunan University, Changsha, Hunan 410082, People's Republic of China

^b Department of Chemical and Biological Engineering, The Hong Kong University of Science and Technology, Clear Water Bay, Kowloon, Hong Kong, China

^c Energy Institute, The Hong Kong University of Science and Technology, Clear Water Bay, Kowloon, Hong Kong, China

^d Research Institute of Chemical Defense, Beijing 100191, China

[†]These authors contributed equally to this work.

Correspondence and requests for materials should be addressed to Y.X. (email: drxiangyu2016@126.com) or X.C. (email: chenxuli@hnu.edu.cn) or H.H. (email: huanghw@hnu.edu.cn).

EXPERIMENTAL SECTION

Materials and Chemicals. Palladium acetylacetonate ($\text{Pd}(\text{acac})_2$), bismuth neodecanoate ($\text{Bi}(\text{C}_{10}\text{H}_{19}\text{O}_2)_3$), polyvinylpyrrolidone (PVP, $M_w = 55\ 000$), commercial Pd/C (10 wt. % of Pd) and Nafion solution (5wt. %) were purchased from Sigma-Aldrich Co. Ltd. N, N-Dimethylacetamide (DMAC) and antimony trichloride (SbCl_3) were purchased from Aladdin Biochemical Technology Co. Ltd. N, N-Dimethylformamide (DMF) and molybdenum hexacarbonyl ($\text{Mo}(\text{CO})_6$) were purchased from Macklin Biochemical Co. Ltd. Lead acetylacetonate ($\text{Pb}(\text{acac})_2$) was purchased from Alfa Aesar. L-ascorbic acid (AA), potassium bromide (KBr), citric acid (CA), ethylene glycol ($\text{C}_2\text{H}_6\text{O}_2$), ethanol ($\text{CH}_3\text{CH}_2\text{OH}$), acetone ($\text{C}_3\text{H}_6\text{O}$), isopropanol ($\text{C}_3\text{H}_8\text{O}$) and potassium hydroxide (KOH) were purchased from Sinopharm Chemical Reagent Co. Ltd. (Shanghai, China). All the chemicals were used without further purification. Ultrapure water (18.2 $M\Omega/\text{cm}$, Master-515Q, HHitech) was used in all our experiments.

Synthesis of ultrathin Pd nanosheets (NSs). 31.5 nm-Pd NSs were prepared by the previously reported method.¹ In a typical experiment, 16 mg of $\text{Pd}(\text{acac})_2$, 90 mg of CA, 30 mg KBr and 30 mg of PVP were dissolved in 10 mL of DMF in a 30 mL reaction flask under magnetic stirring at room temperature. After 1 h, 75 mg of $\text{Mo}(\text{CO})_6$ was added into the homogeneous solution and capped. The as-prepared mixture was then heated and kept at 80 °C for 3h in an oil bath. The resulting products were precipitated by acetone for further use. The Pd NSs with different sizes were obtained via the same method except for varying the amount of KBr to 20 and 35 mg KBr, respectively.

Synthesis of ultrathin Pd-based nanorings (NRs). In a typical synthesis, 1mg of Pd NSs, 2 mg $\text{Bi}(\text{C}_{10}\text{H}_{19}\text{O}_2)_3$, 5mg AA, 30 mg PVP, 2 mL ethylene glycol and 4 mL DMAC were added into a 30 ml reaction flask. After sonicated for 1 h, N_2 was blown over the solution for 10 min. After the vial had been capped, the homogeneous mixture was kept at 140 °C in an oil bath for 3 h under intense stirring and naturally cooled to room temperature. The resulting products were collected by centrifugation at 13, 500 rpm and washed with ethanol for three times. The PdSb, and PdPb NRs were obtained by replacing $\text{Bi}(\text{C}_{10}\text{H}_{19}\text{O}_2)_3$ with SbCl_3 (1.0 mg), and $\text{Pb}(\text{acac})_2$ (1.2 mg) at 140 °C for 0.25, 5 h while keeping other conditions the same, respectively. The PdBiPb trimetallic NRs were obtained via the same method of PdBi NRs except for the addition of $\text{Pb}(\text{acac})_2$ (0.7 mg).

Electrochemical Measurements. Pd NSs or PdBi NRs (20% weight of the catalysts) and Vulcan XC-72R carbon black were dispersed in 2 mL of ethanol under ultrasonication for 1 h.² Subsequently, the Pd NSs or PdBi NRs was dropped in the carbon black under ultrasonication for 2 h. The Pd NSs/C or PdBi NRs/C was collected by centrifugation and then dispersed in 0.99 mL of ethanol and 0.01 mL of Nafion (5wt. %) for several hours to form well-dispersed suspension as catalyst ink. 4 mg of commercial Pd/C was dispersed in 0.75 mL of H₂O, 0.24 mL of isopropanol and 0.01 mL of Nafion (5 wt. %) under ultrasonication for several hours. After that, 0.01 mL of ink was dropped and dried on the glassy carbon electrode (GCE with a diameter of 5 mm) with the loading amount of 3.6 μg , 4.0 μg and 4.0 μg for PdBi NRs, Pd NSs and commercial Pd/C, respectively (determined by ICP-AES).

The electrochemical tests were carried out on a CHI660e electrochemical workstation (Chenhua Instrument, China) via a three-electrode cell system. A glassy carbon electrode was used as the working electrode, the Hg/ HgO electrode was used as a reference electrode, and a platinum wire was used as a counter electrode. All potentials were converted into the values in reference to reversible hydrogen electrode (RHE). The cyclic voltammograms (CVs) were conducted at a scan rate of 50 mV s⁻¹ in N₂-saturated 1 M KOH with and without 1 M ethanol in the potential range of 0.0-1.225 V_{RHE}. The electrochemical active surface areas (ECSAs) were calculated from the CVs obtained in the 1 M KOH by the following formula:

$$\text{ECSA} = \frac{Q}{0.405 * m_{\text{Pd}}}$$

where Q was the integrated charge corresponding to the reduction peak of PdO, m_{Pd} was the Pd loading on the working electrode, and 0.405 mC cm⁻² was the charge value given for the reduce PdO monolayer. The catalytic stability of the as-prepared catalysts was examined via i-t measurements at 0.725 V vs RHE. For CO-stripping measurements, CO gas (99.99%) was first bubbled into the electrolyte at a potential of 0.05 V_{RHE} for 30 min. Then, N₂ gas was fed into the electrolyte to eliminate the dissolved CO, and two complete cycles of CO-stripping curves were recorded at a scan rate of 50 mV s⁻¹. In addition, commercial Pd/C was employed as a reference.

Characterization Techniques. Transmission electron microscopy (TEM) images were taken on a JEOL JEM-2100 operating at an accelerating voltage of 200 kV. High-resolution TEM (HRTEM) characterizations and elemental mapping information were obtained on a JEOL ARM-200F field-emission transmission electron microscope at an accelerating voltage of 200

kV. X-ray photoelectron spectroscopy (XPS) analysis was collected using a Kratos Axis-Ultra DLD instrument with a monochromatized Al K α line source (150 W). To identify the composition of the samples, inductively coupled plasma-atomic emission spectroscopy (ICP-AES) with a SPECTRO BLUE SOP was performed to identify the composition of the samples. X-ray diffraction (XRD) spectra was recorded by using a PANalytical X'pert MPD Pro diffractometer with Ni-filtered Cu K α irradiation (wavelength: 0.15405 nm) in the range from 20° to 90° at the scan rate of 5 deg·min⁻¹.

Density functional theory (DFT) calculations. In this work, all calculations are carried out within the Perdew-Burke-Ernzerhof generalized gradient approximation (GGA)³ with D3 type van der Waals interaction (vdW) correction^{4,5} implemented in Vienna ab initio simulation package (VASP).⁶ The projector augmented wave (PAW) potential⁷ and the plane-wave cut-off energy of 400 eV are used. Our calculations have used a slab model composed of four layers of (3 × 3) supercell for (111) surfaces separated by 20 Å of vacuum space. The 3×3×1 Monk-horst k-point meshes were used for the Brillouin-zone integrations of supercell models. The criteria of convergence were set to 1×10⁻⁵ eV for the self-consistent field (SCF) and 0.02 eV/Å for ion steps. A frequency analysis was carried out on the stable states in order to confirm that these represent genuine minima. All of the electronic energies were corrected for zero-point energy (ZPE) contributions. To explore the free energy profile along the ethanol electro-oxidation pathway, the change in Gibbs free energy for all intermediates has been evaluated using the following relation: $\Delta G = \Delta E - T\Delta S$. Where E is the total energy calculated from DFT and S (entropy) can be obtained directly from a physical chemistry table.

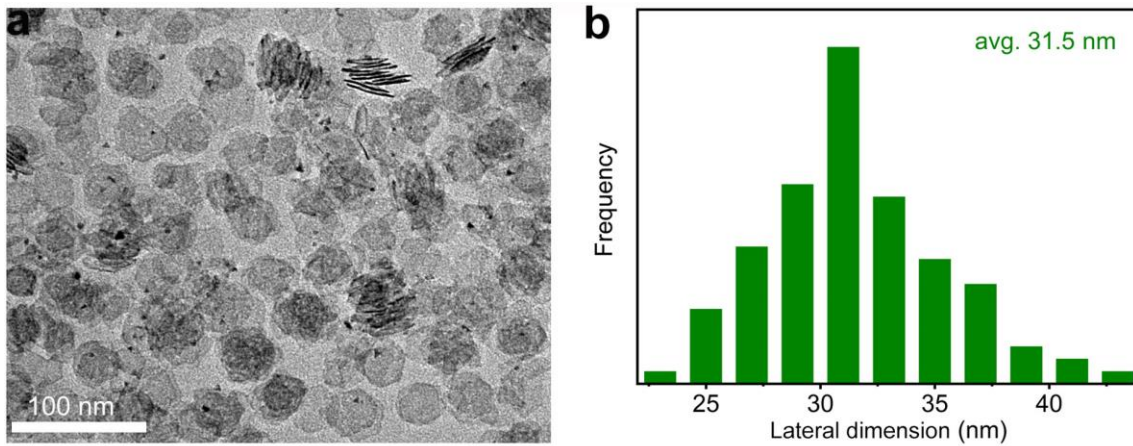


Fig. S1 (a) TEM image and (b) corresponding lateral dimension distribution histogram of 31.5 nm-Pd NSs.

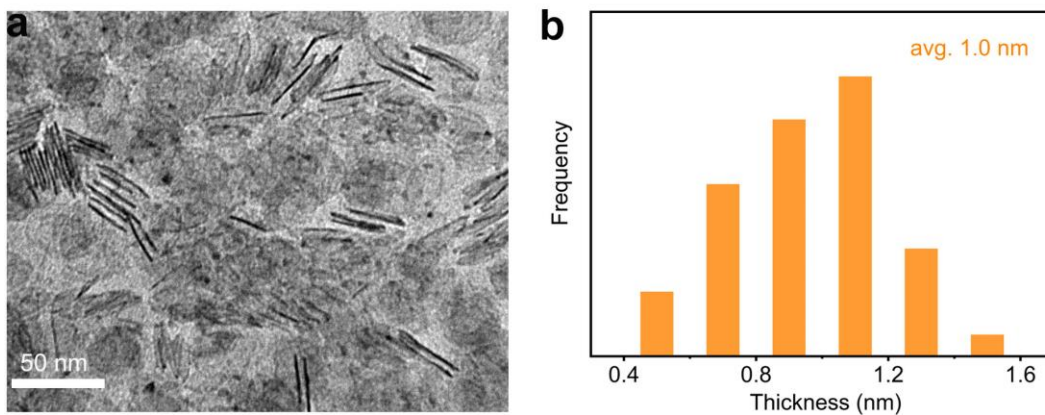


Fig. S2 (a) TEM image and (b) corresponding thickness distribution histogram of 31.5 nm-Pd NSs. The thickness was determined by measuring the vertically standing NSs directly.

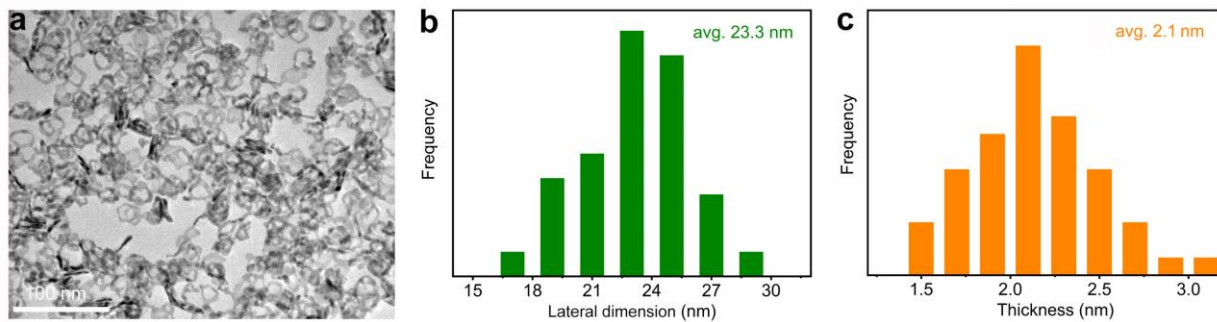


Fig. S3 (a) TEM image of 23.3 nm-PdBi NRs. (b) lateral dimension and (c) thickness distribution histograms of 23.3 nm-PdBi NRs.

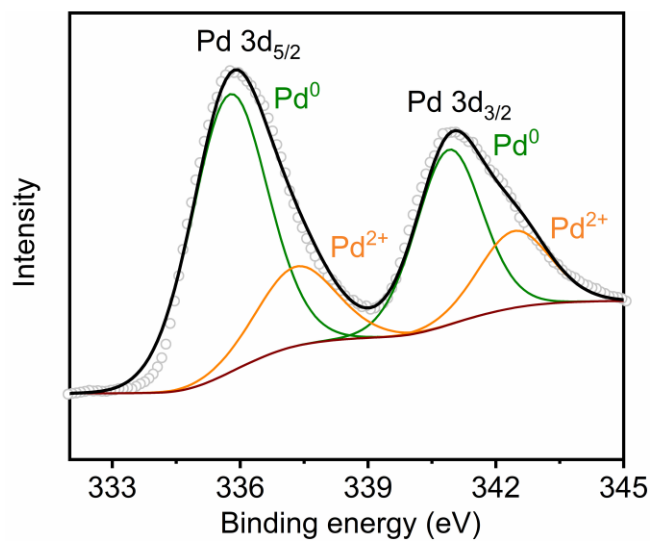


Fig. S4 XPS of Pd 3d spectra of Pd NSs.

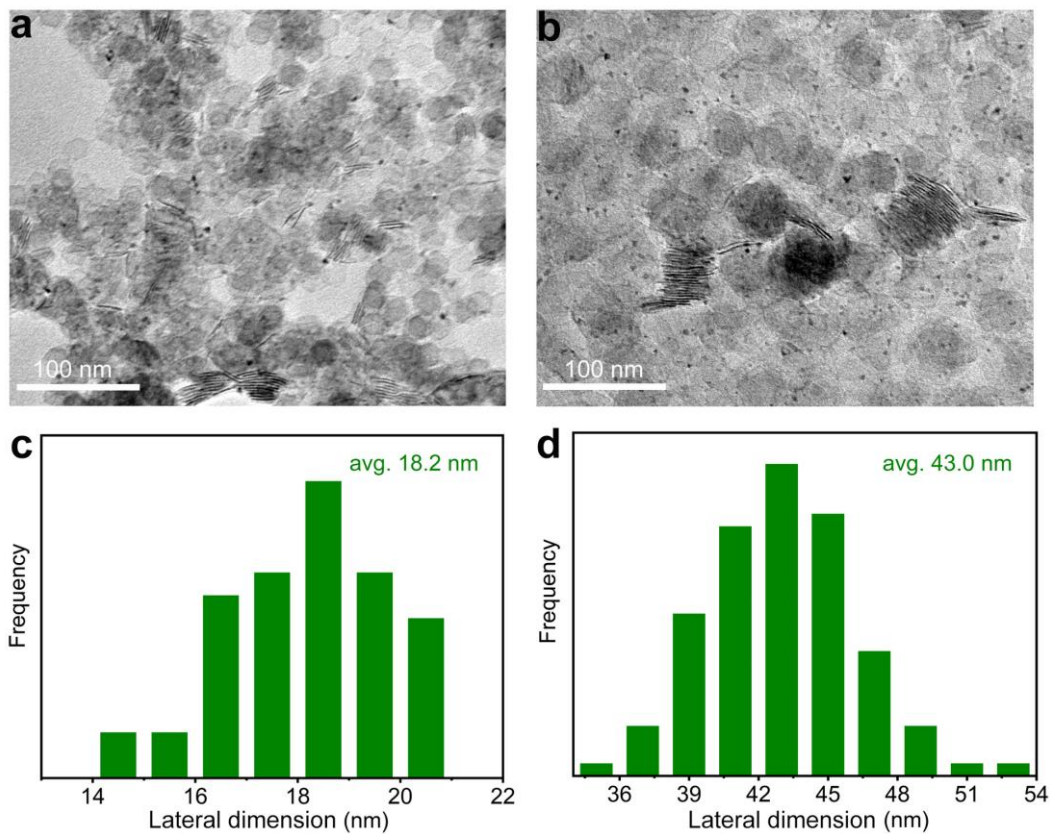


Fig. S5 (a) TEM image and (c) corresponding lateral dimension distribution histogram of 18.2 nm-Pd NSs. (b) TEM image and (d) corresponding lateral dimension distribution histogram of 43.0 nm-Pd NSs.

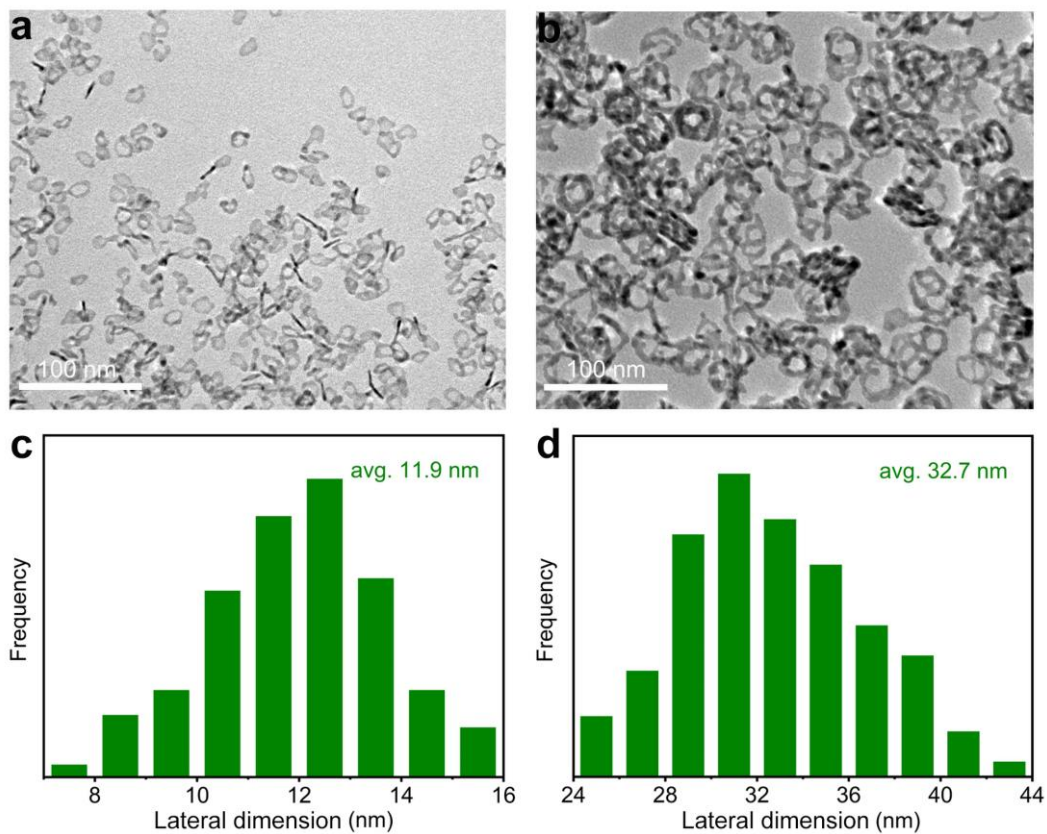


Fig. S6 (a) TEM image and (c) corresponding lateral dimension distribution histogram of 11.9 nm-Pd NRs. (b) TEM image and (d) corresponding lateral dimension distribution histogram of 32.7 nm-Pd NRs.

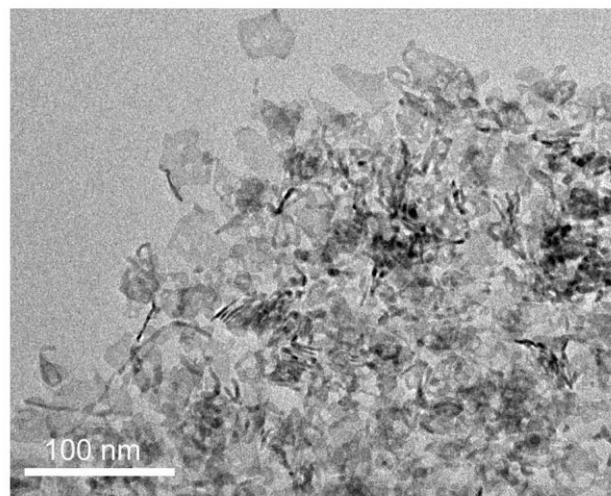


Fig. S7 TEM image of products with the same reaction conditions as that of PdBi NRs but in the absence of $\text{Bi}(\text{C}_{10}\text{H}_{19}\text{O}_2)_3$.

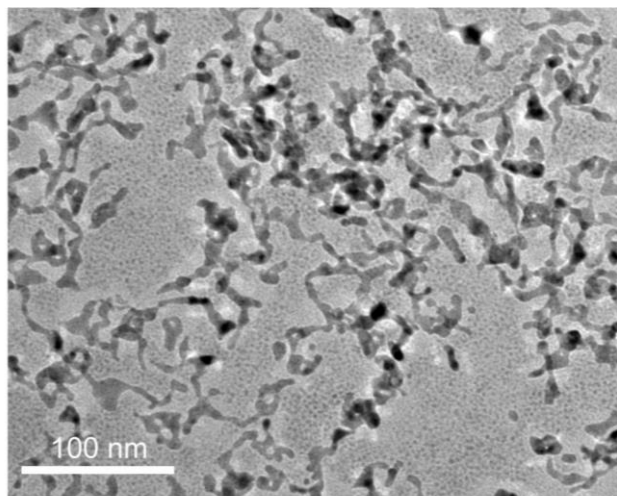


Fig. S8 TEM image of products with the same reaction conditions as that of PdBi NRs except using 3mg $\text{Bi}(\text{C}_{10}\text{H}_{19}\text{O}_2)_3$.

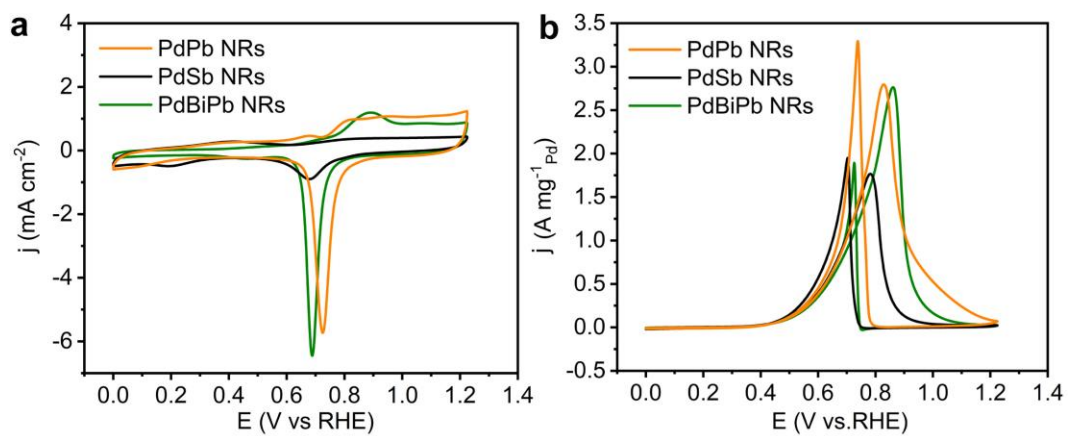


Fig. S9 Electrocatalytic EOR performance of PdPb, PdSb and PdBiPb NRs. (a) CV curves recorded in N_2 -saturated 1 M KOH solution at a scan rate of 50 mV s^{-1} at room temperature. (b) CV curves recorded in N_2 -saturated 1 M KOH solution with 1 M ethanol at a scan rate of 50 mV s^{-1} at room temperature.

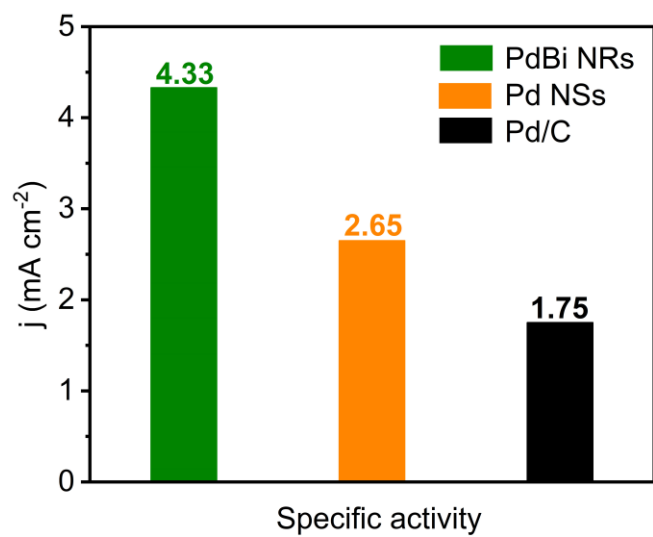


Fig. S10 Specific activities recorded at their corresponding peak potentials in the CV curves.

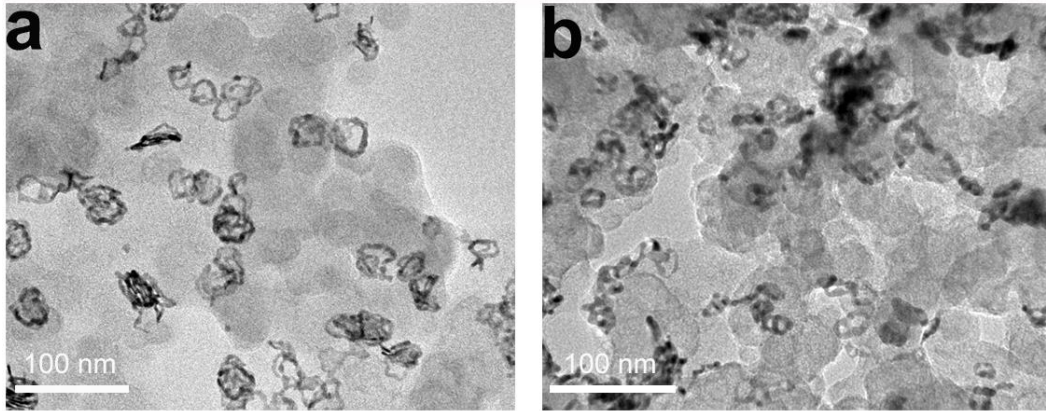


Fig. S11 TEM images of PdBi NRs/C before and after the stability test.

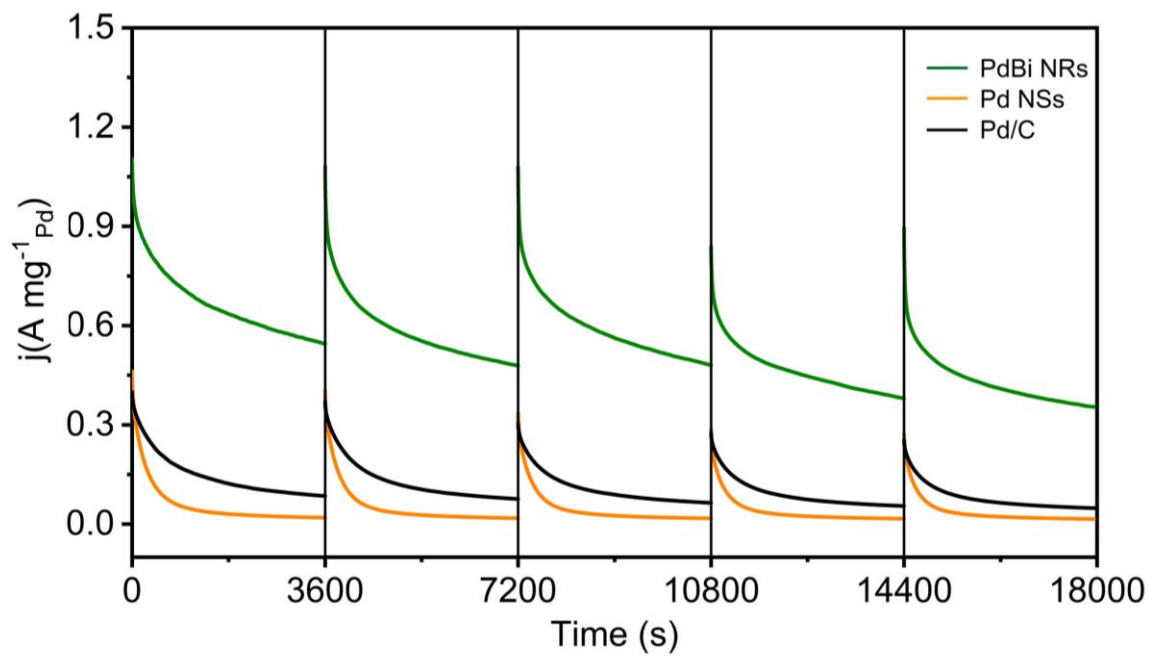


Fig. S12 Long-time durability of PdBi NRs/C, Pd NSs/C and commercial Pd/C in N₂-saturated 1M KOH solution contained 1M ethanol recorded at 0.725 V_{RHE}. After each 3600s stability test, the catalysts were reactivated by sweeping five CV cycles in N₂-saturated 1M KOH.

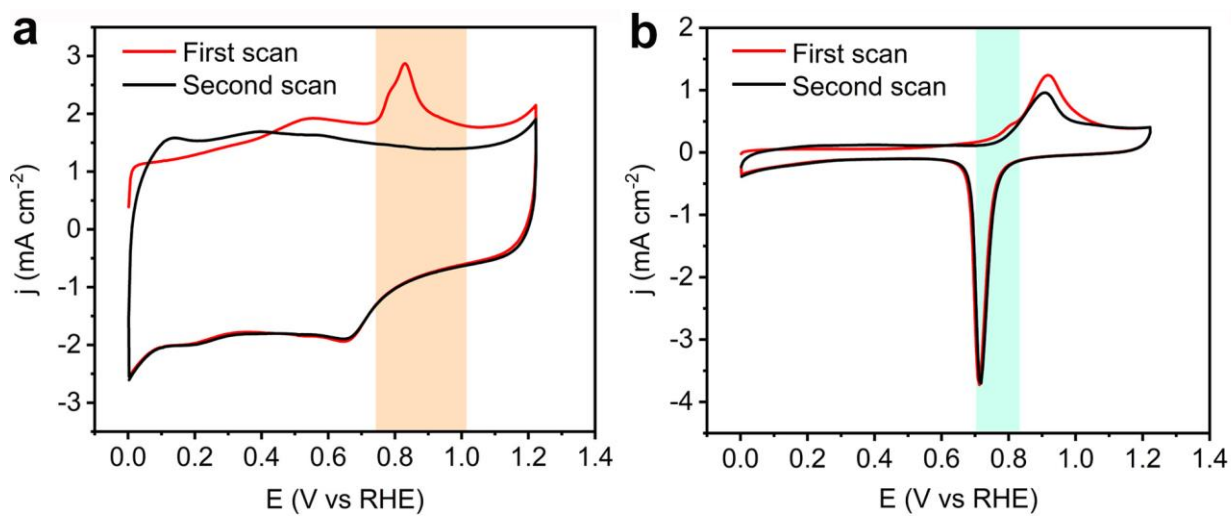


Fig. S13 CO stripping curves of (a) commercial Pd/C and (b) PdBi NRs/C.

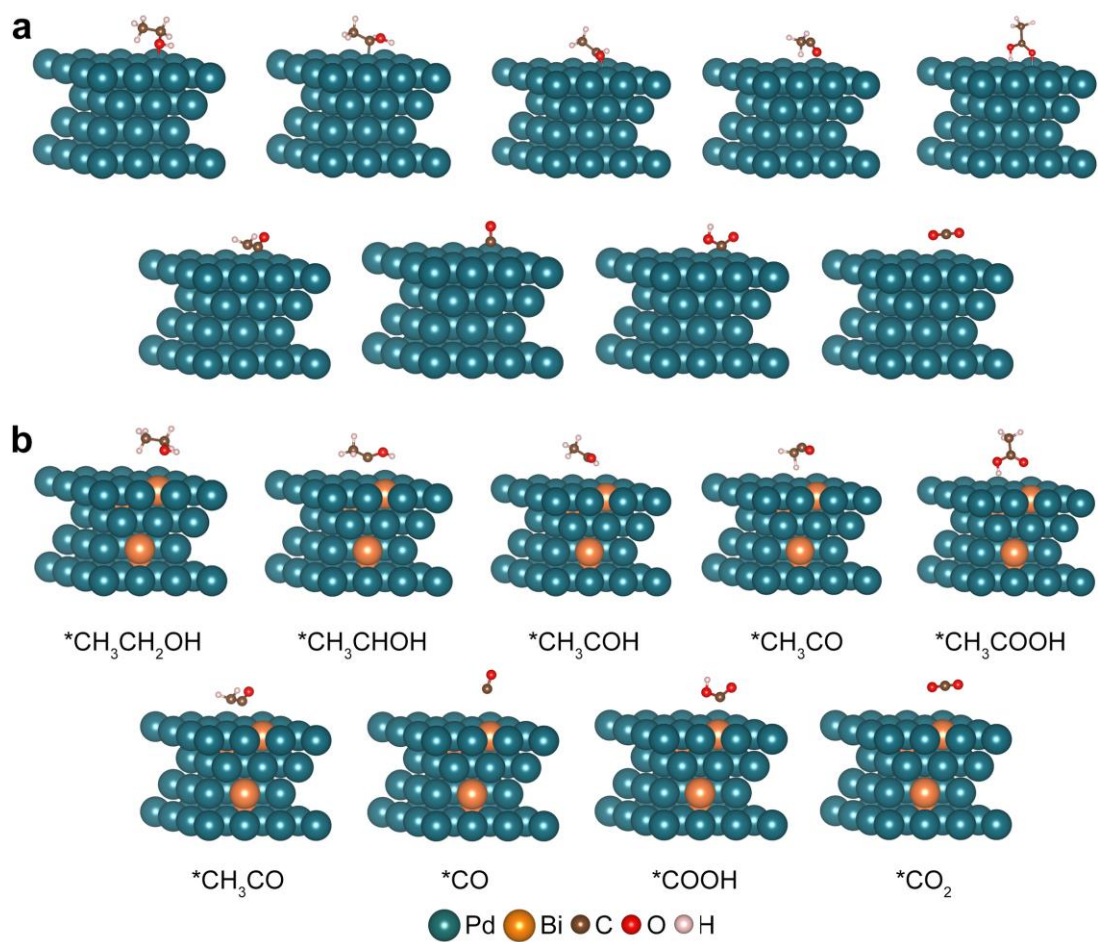


Fig. S14 Adsorption configuration of the intermediates involved in the C₁-path EOR on the (a) Pd and (b) PdBi surfaces.

Table S1. Atomic ratio of as-prepared samples conducted by ICP-AES

Sample	Atomic ratio/%			
	Pd	Bi	Sb	Pb
PdBi	88.3	11.7	—	—
PdSb	93.7	—	6.3	—
PdPb	75.9	—	—	24.1
PdBiPb	75.7	16.4	—	7.9

Table S2. Performance of PdBi/C catalyst in this work and several representative results of other Pd-based bimetallic catalysts from recent published works.

Catalysts	MA (A mg ⁻¹)	Condition	Reference
PdBi NRs/C	3.21	1M KOH +1M CH₃CH₂OH	This work
Pd-Bi(OH) NSs/C	2.20	1M NaOH +0.5M CH ₃ CH ₂ OH	8
PdZn NSs/C	2.73	1M NaOH +1M CH ₃ CH ₂ OH	9
Pd ₃ Bi NPs/C	2.02	1M KOH +1M CH ₃ CH ₂ OH	10
PdAg NDs/C	2.60	1M KOH +1M CH ₃ CH ₂ OH	11
PdCo NTAs/CFC	1.49	1M KOH +1M CH ₃ CH ₂ OH	12
PdCu NPs/C	1.63	1M KOH +1M CH ₃ CH ₂ OH	13
PdAg Networks/C	1.97	1M KOH +1M CH ₃ CH ₂ OH	14
PdAg NWs/C	2.84	1M KOH +1M CH ₃ CH ₂ OH	15
PdSm NCs/C	1.03	1M KOH +1M CH ₃ CH ₂ OH	16
PdIn/C	2.82	1M KOH +1M CH ₃ CH ₂ OH	17

Table S3. Atomic ratio of PdBi nanorings conducted by ICP-AES before and after the stability test.

Sample	Atomic ratio/%	
	Pd	Bi
Initial	88.3	11.7
After 3600 s	89.1	10.9

REFERENCES

- (1) Wang, W., Zhang, X., Zhang, Y., Chen, X., Ye, J., Chen, J., Lyu, Z., Chen, X., Kuang, Q., Xie S., Xie Z, *Nano Lett.* **2020**, *20*, 5458–5464.
- (2) Guo, J., Gao, L., Tan, X., Yuan, Y., Kim, J., Wang, Y., Wang, H., Zeng, Y., Choi, S.-Il., Smith, S.C., Huang, H, *Angew. Chem. Int. Ed.* **2021**, *60*, 10942-10949.
- (3) Perdew, J. P.; Burke, K.; Ernzerhof, M, *Phys. Rev. Lett.* **1996**, *77*, 3865–3868.
- (4) Grimme, S.; Antony, J.; Ehrlich, S.; Krieg, S, *J. Chem. Phys.* **2010**, *132*, 154104.
- (5) Grimme, S.; Ehrlich, S.; Goerigk, L, *J. Comp. Chem.* **2011**, *32*, 1456–1465.
- (6) Kresse, G.; Furthmüller, J, *Phys. Rev. B* **1996**, *54*, 11169–11186.
- (7) Blöchl, P. E, *Phys. Rev. B* **1994**, *50*, 17953–17979.
- (8) M. Chu, J. Huang, J. Gong, Y. Qu, G. Chen, H. Yang, X. Wang, Q. Zhong, C. Deng and M. Cao, *Nano Res.*, 2022, **15**, 3920-3926.
- (9) Q. Yun, Q. Lu, C. Li, B. Chen, Q. Zhang, Q. He, Z. Hu, Z. Zhang, Y. Ge and N. Yang, *ACS Nano*, 2019, **13**, 14329-14336.
- (10) X. Lao, M. Yang, X. Sheng, J. Sun, Y. Wang, D. Zheng, M. Pang, A. Fu, H. Li and P. Guo, *ACS Appl. Energy Mater.*, 2022, **5**, 1282-1290.
- (11) W. Huang, X. Kang, C. Xu, J. Zhou, J. Deng, Y. Li and S. Cheng, *Adv. Mater.*, 2018, **30**, 1706962.
- (12) A. L. Wang, X. J. He, X. F. Lu, H. Xu, Y. X. Tong and G. R. Li, *Angew. Chem. Int. Ed.*, 2015, **54**, 3669-3673.
- (13) J. Xue, G. Han, W. Ye, Y. Sang, H. Li, P. Guo and X. S. Zhao, *ACS Appl. Energy Mater.*, 2016, **8**, 34497-34505.
- (14) S. Fu, C. Zhu, D. Du and Y. Lin, *ACS Appl. Energy Mater.*, 2015, **7**, 13842-13848.
- (15) H. Lv, Y. Wang, A. Lopes, D. Xu and B. Liu, *Appl. Catal. B: Environ.*, 2019, **249**, 116-125.
- (16) G. Zhang, Y. Wang, Y. Ma, Y. Zheng, H. Zhang, M. Tang and Y. Dai, *Catal. Today*, 2023, **409**, 63-70.
- (17) Y.-J. Chen, Y.-R. Chen, C.-H. Chiang, K.-L. Tung, T.-K. Yeh and H.-Y. Tuan, *Nanoscale*, 2019, **11**, 3336-3343.